International Journal of Recent Technology and Engineering (IJRTE)
ISSN: 2277-3878 (Online), Volume-9 Issue-4 November 2020

Measurement of Slice Thickness of a Medical Image using a Wedge Phantom

Cheolpyo Hong

Abstract*: Slice thickness measurement is an essential parameter of performance evaluation for the medical imaging system. This study demonstrates the characteristics of slice thickness measurement for medical images using a wedge digital phantom. A wedge-shaped digital phantom was generated and the ideal edge response function (ERF) was extracted from line profile in single slice. The corresponding slice profile was calculated by the derivative of ERF. The wedge phantom obtained by applying gaussian convolving to a digital phantom was also generated to produce similarities to real medical images. Unlike an ideal slice profile, it was estimated by the full width half maximum (FWHM) of the Gaussian function fitting. In addition, we evaluate the effect of background noise and wedge angle for the wedge phantom. The estimated FWHM of the image with noise added was increased by 10.4% compared to the image without noise. However, the FWHM from the line profiles averaging on the noise-added image was estimated by 0.2% reduction than the noise-free image. The line profiles averaging improves the accurate measurement of slice thickness by decreasing the noise. Despite the wedge angle changing from 45 to 30 degrees, the resulting FWHM was estimated to have less than 1% difference. However, the length of the line profile to be acquired should be increased as the wedge angle increases.

Index Terms: Extended field of view, seamless image, image stitching, geometric distortion, open MRI.

I. INTRODUCTION

Medical imaging systems utilize spatial resolution in order to distinguish various objects, such as small objects of human tissue that can be clearly distinguished on high-resolution medical images [1-4]. The spatial resolution depends on the size of the pixel, which is the value for the image size divided by the matrix size. The pixels in-plane of medical images are composed of rows and columns. A medical image is a two-dimensional (2D) representation of a three-dimensional (3D) object, yet the 2D image can have depth depending on the certain slice thickness and is a sum of depth information [5-7]. The 2D image degradation is generated by the intrinsic resolution limit of the imaging system. 2D image degradation can be generated by the intrinsic resolution limit of the imaging system used. In particular, partial volume effects can be easily observed in medical images, which can be defined as the partition of the identical object because of the intrinsic resolution limit [8-12]. The single pixel intensity can appear as several pixels depending on the spatial resolution used. Such an effect can generate the distortion of geometric and intensity information for human tissue. Partial volume artifacts can also be created due to variations and imperfections inherent within medical imaging systems [13,14]. For instance, a 2D image with a 5mm slice thickness can appear as a 7mm slice thickness image, because of imperfections within slice selection RF pulses in magnetic resonance imaging (MRI) equipment. The acquired image can be generated differently from the setup of the user. It is especially difficult to recognize partial volume artifacts in the slice direction in 2D images. The accurate measurement of slice thickness is an important parameter of performance evaluation for medical imaging systems [5,15,16]. However, the comprehensive characteristics of slice thickness measurement are not well described. In this study, we demonstrate the characteristics of slice thickness measurement for medical images using a wedge digital phantom. The edge response function (ERF) was extracted from line profile of wedge image. The slice thickness was calculated by the derivative of ERF. We also evaluate the effect of background noise in images and wedge angles for the wedge phantom.

Revised Manuscript Received on November 20, 2020.
***** Correspondence Author
Cheolpyo Hong*, Department of Radiological Science, Daegu Catholic University, Daegu, Republic of Korea. Email: chong@cu.ac.kr

II. MATERIALS AND METHOD

A. Wedge phantom image acquisitions

For this study, a binary image with 0 and 255 intensity was generated as a wedge-shaped digital phantom, shown in Figure 1(a). The image has a 256 × 256 matrix. The vertical and horizontal direction of the image indicates slice-direction (z) and the image plane (x). The wedge angle (θ) was set at 45 degrees. The slice thickness was selected as the value of 30 lines on 256 vertical lines. So, the reference slice thickness was a value of 30.

B. Slice thickness measurement

Slice thickness measurement was accomplished by an edge response function (ERF) of the wedge's line profile (Fig. 1(b)). The derivative of the ERF indicates the ideal slice profile that was projected at the selected slice thickness by the angle of wedge (θ), shown in Figure 1(c). However, the derivative of the ERF indirectly represents the slice profile of a real medical image because of margin uncertainty, shown in Figure 2(b). As a result, the slice thickness was defined as follows:

$$\text{Slice thickness} = FWHM \times \tan\theta$$

The slice thickness was estimated by the full width half maximum (FWHM) from the Gaussian function fitting.

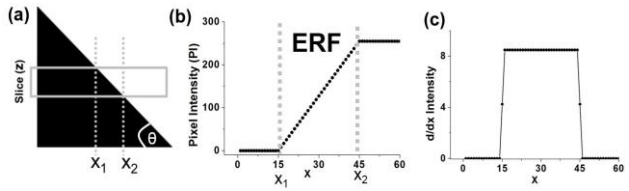

Figure 1. A wedge-shaped digital phantom (a) and selected slice width (gray box). The vertical shows slice-direction (z) and the horizontal shows the image plane (x). The angle (θ) and the slice thickness was set at 45 degrees and the value of 30 arbitrary units (au). (b) Illustration of the ideal edge response function (ERF) of line profile in selected slice. (c) The derivative of ERF was shown in the form of a box.

C. The effects of noise and wedge angle.

The wedge image was also obtained by applying gaussian convolving to a digital phantom to create similarities to real medical images, shown in Figure 2(a). The convolution operations with a Gaussian offers higher weight to margin pixels than non-margin pixels inside the image. Therefore, the uncertainty of the margin increased in Figure 2(b) compared to Figure 1(b). The standard deviation sigma of the Gaussian was set to a value of 2. In addition, a background noise-added image was generated to evaluate the noise effect for slice thickness calculation. A Gaussian noise with a standard deviation of 3 was applied on the wedge image. To assess the impact of noise, different ERFs were selected, shown in Figure 3. We compared the single line profile with the average value of 30 consecutive profiles. The effects of wedge angles were also evaluated. A wedge image with an angle of 30 degrees was generated. The Gaussian convolving and background noise were also applied to the wedge image. As the wedge angle was set at 45 and 30 degrees, the corresponding tangent values were assigned 1 and 0.57

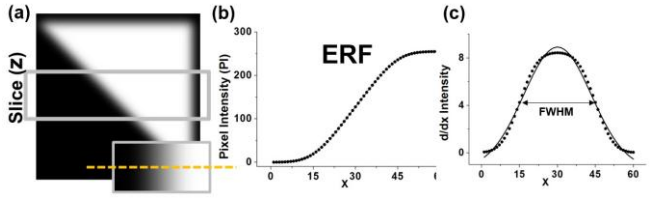

Figure 2. (a) The wedge phantom obtained by applying Gaussian convolving to a digital phantom of Fig. 1(a). The lower right figure is the resulting plane image of the selected slice (yellow line shows selected line profile). (b) Illustration of the edge response function (ERF) of line profile. (c) The derivative of ERF was shown in the form of a Gaussian curve. The solid line was obtained by Gaussian function fitting. FWHM denotes full width at half maximum.

III. RESULTS

The derivative of the ideal ERF was a value of 30, which is the reference slice thickness shown in Figure 1(c). The margin of the ERF was clearly defined and the corresponding slice profile was suitably calculated. However, Figure 2 shows that the margin of the ERF was not appropriately defined in the Gaussian convolving image. The corresponding slice profile was estimated at a value of 31.3 from the FWHM of Gaussian curve fitting, shown in Figure 2(c).

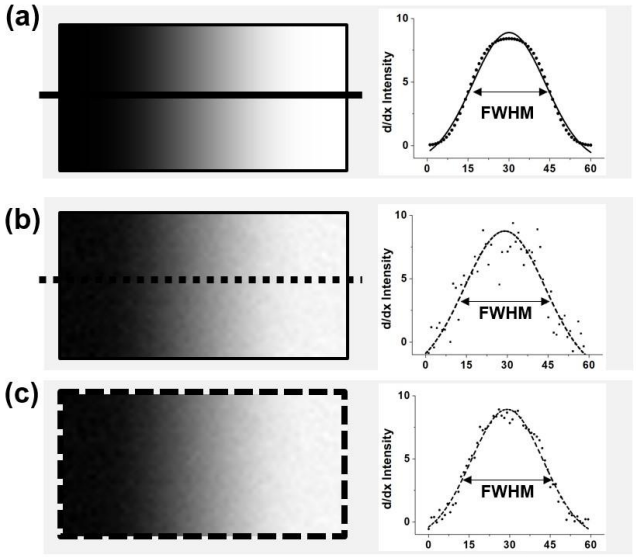

Figure 3. (a) The resulting image from the selected slice width of wedge and the corresponding estimated slice profile. The solid line was obtained by Gaussian function fitting of ERF from line profile. (b) The noise-added image with above image (a) and the corresponding estimated slice profile. (c) The noise-added image with above image (b). For the image, 30 consecutive profiles were obtained and averaged. The slice profile was estimated by the ERF generated from the average line profile.

Figure 3 shows the noise-added image and the corresponding estimated slice profile. The estimated FWHM was as a value of 34.9 for the noise added image. As the background image noise was added, the inaccuracy of the slice thickness was increased by 10.4%. However, the estimated FWHM of the noise-added image was a value of 31.6 through the line profile averaging method. This value was calculated by a 0.2% reduction than the noise-free image.

The wedge phantom image with a 30 degrees angle is shown in Figure 4. The estimated FWHM was a value of 54.3, and the calculated slice thickness was a value of 31.4. This value was calculated as the product of FWHM and tangent values, with the FWHM widening as the angle is reduced.

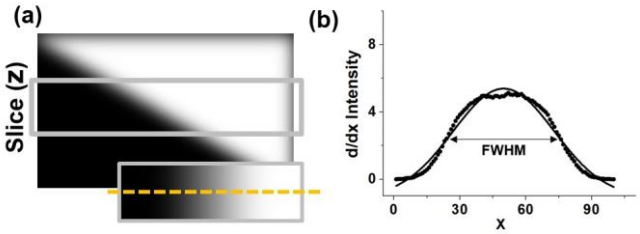

Figure 4. (a) The wedge phantom obtained by applying Gaussian convolving to a digital phantom of Fig. 1(a). The angle (θ) and the slice thickness was set at 30 degrees and the value of 30 arbitrary units (au). The lower right figure is the resulting image of the selected slice (yellow line shows selected line profile). (b) The corresponding estimated slice profile. The FWHM widened because the angle was reduced.

IV. DISCUSSION

The ideal ERF has sharp edges and is easily distinguished for the wedge margin. The corresponding slice profile was calculated as a reference value. However, actual medical images are affected by various factors such as background noise, the setup parameters, and object characteristics. As a result, the wedge margin becomes uncertain and the slice thickness is estimated by the FWHM through Gaussian curve fitting. Medical images include background noise, inevitably causing errors in measuring the slice thickness. In this study, the slice thickness measurement generated a 10.4% error even when containing noise that is not visually prominent. However, such an error can be reduced according to the processing method of noise. Line profile averaging reduced the measurement error to 0.4%. which should allow for an accurate measurement of slice thickness.

Slice thickness measurement is not affected by the wedge angle, shown in Figure 4. However, the stretch effect should be considered because of the impacts associated with a widening angle. The slice thickness is widely projected on the image section. When the angle is reduced from 45 degrees to 30 degrees, the value of FWHM increases by 72%. As a result, a wide range field-of-view (FOV) should be selected for slice thickness calculations. However, the quality of medical images can be altered through changing the FOV. Increasing the FOV increases the signal to noise ratio (SNR) without changing the pixel size, which reduces the spatial resolution. In addition, increasing the spatial resolution increases the length of the image scan time. Finally, if a shorter FOV is selected a Gassing fitting error may occur. The slice thickness should be measured considering those relationships.

V. CONCLUSION

This study demonstrated the characteristics of slice thickness measurement using a wedge digital phantom. The slice thickness is estimated by the derivative of ERF of line profile of wedge images regardless of wedge angles. In addition, it may be possible for slice thickness measurements to be affected by background noise and any noise reduction method applied.

REFERENCES

1. Lagalla, Roberto, and Massimo Midiri., (1998) Image quality control in breast ultrasound, Eur J Radiol., 27: S229-S33
2. Lin E, Alessio A, (2009) What are the basic concepts of temporal, contrast, and spatial resolution in cardiac CT?, J Cardiovasc Comput Tomogr., 3: 403-08
3. Link TM, Majumdar S, Peterfy C, Daldrup HE, Uffmann M, Dowling C, Steinbach L, Genant HK, (1998) High resolution MRI of small joints: impact of spatial resolution on diagnostic performance and SNR, Magn Reson Imaging., 16: 147-55
4. Van Reeth E, Tham I W, Tan C H, Poh C L, (2012) Super-resolution in magnetic resonance imaging: a review, Concepts Magn. Reson. Part A, 40: 306-25
5. Chen C-C, Wan Y-L, Wai Y-Y, Liu H-L, (2004) Quality assurance of clinical MRI scanners using ACR MRI phantom: preliminary results, J Digit Imaging., 17: 279-84
6. Luppino F S, Grooters E, de Bruïne F T, Zwinderman A H, van der Mey A G, (2006) Volumetrical measurements in vestibular schwannoma, the influence of slice thickness and patient's repositioning, Otol Neurotol, 27: 962-68
7. Polacin A, Kalender W A, Brink J, Vannier M A, (1994) Measurement of slice sensitivity profiles in spiral CT, Med Phys., 21: 133-40
8. Ballester M Á G, Zisserman A P, Brady M, (2002) Estimation of the partial volume effect in MRI, Med Image Anal., 6: 389-405
9. Bullmore E, Brammer M, Rouleau G, Everitt B, Simmons A, Sharma T, et al, (1995) Computerized brain tissue classification of magnetic resonance images: a new approach to the problem of partial volume artifact, Neuroimage, 2: 133-47
10. Glover G, Pelc N, (1980) Nonlinear partial volume artifacts in x-ray computed tomography, Med Phys., 7: 238-48
11. Kuhnigk J-M, Dicken V, Bornemann L, Bakai A, Wormanns D, Krass S, et al, (2006) Morphological segmentation and partial volume analysis for volumetry of solid pulmonary lesions in thoracic CT scans, IEEE Trans Med Imaging., 25: 417-34
12. Müller-Gärtner H W, Links J M, Prince J L, Bryan R N, McVeigh E, Leal J P, et al, (1992) Measurement of radiotracer concentration in brain gray matter using positron emission tomography: MRI-based correction for partial volume effects, J Cereb Blood Flow Metab., 12: 571-83
13. Kaur P, Kumaran S S, Tripathi R, Khushu S, Kaushik S, (2007) Protocol error artifacts in MRI: sources and remedies revisited, Radiography, 13: 291-306
14. Monnin P, Sfameni N, Gianoli A, Ding S, (2017) Optimal slice thickness for object detection with longitudinal partial volume effects in computed tomography, J Appl Clin Med Phys., 18: 251-59
15. K anzawa T, Ohkubo M, Kondo T, (2017) Measurement of thin slice thickness in MRI using an improved wedge method. European Congress of Radiology 2017.
16. Murphy B, Carson P L, Ellis J H, Zhang Y, Hyde R J, Chenevert T L, (1993) Signal-to-noise measures for magnetic resonance imagers, Magn Reson Imaging., 11: 425-28

AUTHORS PROFILE

Cheolpyo Hong, Assistant Professor, Department of Radiological Science, Daegu Catholic University, Daegu, Republic of Korea. Dr. Hong has received Ph.D. in MRI sequence and geometric distortion correction from Yonsei University, Kwangwon-do. His research interests are MRI guided radiation therapy and Quantitative Imaging. He has 10 years of Teaching Experience in Radiological Science and Published 25 articles in various journals and international conferences.